

Attention Debiasing for Token Pruning in Vision–Language Models

Kai Zhao, Wubang Yuan, Yuchen Lin, Liting Ruan, Xiaofeng Lu, Deng-Ping Fan, Ming-Ming Cheng, Dan Zeng*

Abstract—Vision–language models (VLMs) typically encode substantially more visual tokens than text tokens, resulting in significant token redundancy. Pruning uninformative visual tokens is therefore crucial for improving computational efficiency, and language-to-vision attention has become a widely used importance criterion for this purpose. However, we find that attention in VLMs is systematically biased: it disproportionately favors tokens appearing later in the sequence (manifesting as over-attention to lower image regions) and assigns inflated scores to semantically empty padding tokens. These behaviors stem from intrinsic recency bias and attention sink effects inherited from large language models (LLMs), and they distort attention-based pruning by preserving irrelevant visual content. To derive a pruning criterion better aligned with semantic relevance, we introduce two lightweight yet effective debiasing techniques that restore the reliability of attention. The first compensates for positional distortions by removing recency-induced attention trends, producing a content-aware and position-agnostic importance measure. The second suppresses attention sink effects by eliminating spurious attention on padding tokens. Our method is model-agnostic, pruning-method-agnostic, and task-agnostic, enabling plug-and-play integration with existing VLM pruning models. Despite its simplicity, our approach consistently delivers strong performance gains. We evaluate our method on ten vision–language benchmarks spanning both image- and video-based tasks, in comparison with seven state-of-the-art visual token pruning methods and across two representative VLM architectures. Our method consistently achieves substantial performance gains, demonstrating strong effectiveness and generalizability. Our code is available at <https://github.com/intcomp/attention-bias>.

Index Terms—Vision–Language Models, Token Pruning, Attention Bias, Attention Sink

I. INTRODUCTION

VISION-language models (VLMs) [36], [64], [3], [50] have achieved remarkable progress across a wide range of multimodal tasks, including image captioning [51], [30], visual question answering [14], [45], and complex visual reasoning [29], [34]. Their strong cross-modal alignment and scalable architectures have enabled widespread adoption in both research and real-world applications. Despite these advances, VLMs still suffer from high computational cost and

* Dan Zeng is the corresponding author.

Kai Zhao, Wubang Yuan, Liting Ruan, Xiaofeng Lu and Dan Zeng are with the School of Communication and Information Engineering, Shanghai University. Yuchen Lin is with the School of Computer Science and Engineering, Shanghai University, Shanghai, 200444, China. Email: kz@kaizhao.net, {wubangyuan, litingruan, luxiaofeng, yuchenlin, dzeng}@shu.edu.cn.

Deng-Ping Fan and Ming-Ming Cheng are with the School of Computer Science and Engineering, Nankai University, Tianjin, 300350, China. Email: {fdp, cmm}@nankai.edu.cn.

Manuscript received on January 19, 2026.

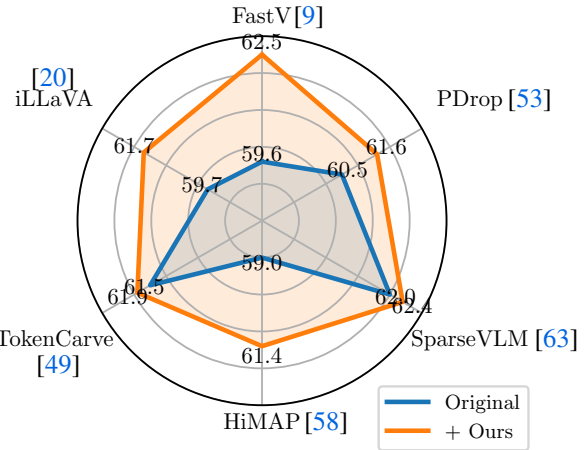


Fig. 1. Average performance of multiple VLMs across ten image-based vision–language QA benchmarks, where each vertex corresponds to a pruning method. Our method consistently improves performance across all six pruning methods.

slow inference [43], [6], [9]. The primary bottleneck arises from the large number of visual tokens. Most VLMs encode images and text separately, and then concatenate their tokens before feeding them into a large language model (LLM) decoder [36], [64], [3]. Due to the inherent redundancy of visual signals, visual tokens greatly outnumber text tokens, creating substantial computational overhead and inefficient inference [9], [8].

To reduce this overhead, recent studies explore *visual token pruning* [43], [6], which aims to remove visual tokens that are irrelevant to the textual input. A widely used strategy relies on language-to-vision attention: visual tokens receiving higher attention are presumed more semantically aligned with the text, while low-attention tokens can be discarded with minimal impact on performance [9], [53], [63], [58], [49], [20].

However, emerging evidence reveals that LLMs exhibit pathological attention behaviors. First, LLMs are known to possess a strong *recency bias*, consistently favoring tokens that appear later in the sequence [18], [60]. This aligns with findings in cognitive and psychological sciences that human cognition tends to better retain more recent events [40], [19]. In VLMs, recency bias manifests as disproportionately high attention on visual tokens located near the bottom of the image. Second, the *attention sink* phenomenon causes the model to assign abnormally large attention scores to semantically empty tokens, such as the *Begin-of-Sequence (BOS)* token [16], [4]. We observe that the same issue appears in VLMs: the decoder

frequently allocates inflated attention to the padding regions of the input image, even though these regions contain no valid visual content. Both *recency bias* and *attention sink* distort the language-to-vision attention, causing pruning algorithms to retain uninformative or text-irrelevant visual tokens.

Recency bias is a common and intrinsic characteristic of large language models (LLMs), arising from their sequential training data and next-token prediction objectives [37], [17]. A recent work [11] has shown that attenuating or removing the influence of Rotary Positional Embedding (RoPE) [47] can effectively alleviate recency bias. Nevertheless, recency bias fundamentally originates from the intrinsic modeling and optimization properties of LLMs [37], [17], and thus cannot be fully eliminated solely by modifying positional encoding schemes [18]. Another line of recent work such as Vis-Pruner [60] attempts to bypass recency bias in text-to-vision attention by pruning tokens using only visual information. However, such approaches ignore cross-modal relevance and thus cannot reliably identify visual tokens most pertinent to the language input.

To address these attention biases and to derive a pruning criterion better aligned with semantic relevance, we propose two extremely simple yet highly effective techniques. First, to remove recency bias, we statistically model the positional trend of attention using large-scale data and construct an exponential recency-bias function. By normalizing attention with this learned function, we obtain a position-agnostic, content-dependent importance criterion. Second, to eliminate attention sink in the padding image area, we simply zero out the attention scores of padding visual tokens, ensuring that no padding region is preserved during pruning. With the proposed two debiasing mechanisms, our method effectively improves the reliability of language-to-vision attention and yields consistent performance gains for existing attention-based visual token pruning methods.

Extensive experiments on ten image-based and three video-based vision–language benchmarks, across multiple VLM architectures, demonstrate that our approach consistently and significantly improves six representative attention-based visual token pruning methods. As summarized in Fig 1, which reports average performance over ten image-based benchmarks, our debiasing technique yields consistent gains across all evaluated pruning methods. Overall, our method exhibits the following favorable properties:

- **Simplicity and efficiency:** It is easy to implement and incurs negligible additional computational overhead.
- **Training-free and plug-and-play:** The module requires no retraining and can be seamlessly integrated into arbitrary attention-based pruning methods on the fly.
- **Consistent effectiveness:** It delivers consistent and substantial performance improvements over existing methods across different models and benchmarks.

The rest of this paper is organized as follows: Sec II summarizes the related works. Sec III elaborates the debiasing method. Sec IV presents experimental details and reports comparison results. Sec V concludes the paper.

II. RELATED WORK

A. Large Vision-Language Models

Large vision–language models (VLMs) integrate powerful vision encoders with large language models to enable multimodal reasoning across tasks such as visual question answering, image captioning, and multimodal dialogue. Despite their strong performance, VLMs suffer from significant computational inefficiency, largely due to the large number of visual tokens produced by vision encoders. Unlike text, where token lengths are typically modest, images are commonly represented by hundreds or even thousands of patch tokens, resulting in substantial quadratic complexity in cross-modal attention.

Early efforts in efficient transformer design addressed token redundancy primarily in unimodal settings. Methods such as Compressive Transformers [42] and Funnel-Transformer [10] reduced sequence length by compressing historical or intermediate representations, demonstrating that deep transformer layers do not require full token resolution. In the vision domain, DynamicViT [43] and SpViT [28] showed that many visual tokens contribute little to final predictions and can be dynamically pruned during inference. Token merging approaches, such as ToMe [6], further revealed that redundant visual tokens can be merged rather than dropped, achieving substantial speedups with minimal accuracy degradation.

As VLMs inherit both the scale and redundancy of their unimodal counterparts, these observations have motivated extensive research into visual token reduction tailored to multimodal inference. Recent VLMs such as LLaVA [36], LLaMA-VID [32], and their variants demonstrate that aggressive visual token compression is feasible, and in some cases even beneficial, provided that essential semantic information is preserved.

B. Visual-Token Reduction in VLMs

Early VLM acceleration methods primarily relied on model retraining or auxiliary learnable modules. For example, FastV [9] prunes visual tokens after early transformer layers using learned importance predictors, while LLaVA-PruMerge [44] combines attention-based token selection with token merging through additional training. Similarly, Sparse-VLM [63] introduces sparsification-aware training to reduce visual token counts during inference.

To avoid retraining large models, a growing body of work has focused on *training-free* visual token pruning. Fit-and-Prune [56] derives pruning configurations by matching attention statistics before and after pruning, enabling rapid deployment without modifying model parameters. VTC-CLS [52] demonstrates that the vision encoder’s [CLS] token provides sufficient global importance cues to identify dispensable visual tokens. HiRED [2] and EVIT [12] similarly exploit attention patterns to guide token dropping without additional training.

Several methods incorporate language guidance to improve pruning decisions. LVPruning [48] uses cross-modal attention to measure the contribution of each visual token to the textual context, discarding tokens with minimal language relevance. IVTP [22] further introduces instruction-aware pruning by

considering both visual saliency and query relevance. ATP-LLaVA [57] adaptively adjusts pruning ratios based on multi-modal interactions during inference.

Another line of research emphasizes diversity-aware and structure-aware pruning. DivPrune [1] formulates token selection as a diversity maximization problem to avoid retaining redundant visual information. Graph-based approaches, such as KIND [26], model visual tokens as nodes in a similarity graph and select influential tokens through graph propagation. Beyond attention or similarity heuristics, conditional diversity-based pruning [61] explicitly balances relevance and diversity conditioned on language queries.

Hierarchical and progressive token reduction strategies have also been explored. Conical visual concentration [53] prunes tokens stage by stage, retaining full resolution in early layers while gradually increasing sparsity. Dynamic-LLaVA [23] and ST3 [65] further incorporate spatial and temporal cues to support adaptive pruning in both image and video settings.

Complementary to pruning, extreme token compression methods demonstrate that only a handful of visual tokens may suffice. LLaMA-VID [32] compresses each image or video frame into two tokens, while LLaVA-Mini [62] represents visual input using a single token. TokenPacker [31] and VisionZip [55] similarly reduce visual token counts via efficient projection and selection mechanisms. Matryoshka-style models [7], [21] enable flexible inference by producing nested representations that support variable token budgets.

Overall, the evolution of visual token reduction in VLMs reflects a clear trend from retraining-based sparsification toward lightweight, training-free, and plug-and-play pruning strategies. However, existing methods overlook or bypass the systematic attention biases inherent in LLMs, which can mislead attention-based pruning criteria.

III. METHODOLOGY

Our method explicitly addresses two dominant sources of bias in attention-based visual token pruning—recency bias and attention sink on padding regions—by introducing *positional debiasing* and *padding attention suppression*, respectively.

A. Positional Debiasing

Let $a_i \in \mathbb{R}^+$ be the attention score of a language token to the i -th visual token, averaged over multiple attention heads. The specific definition of a_i depends on the chosen baseline pruning method, which determines how language-to-vision attention is computed.

Recent studies show that VLMs exhibit a strong recency bias [60], where later visual tokens consistently receive higher attention. As illustrated in Fig 2, the raw attention score rises sharply with token index, indicating a content-agnostic bias toward lower image regions. Such bias misleads pruning by preserving visually uninformative tokens purely due to their positions.

To separate content-agnostic bias from content-dependent attention, we decompose the attention score as

$$a_i = b_i \cdot \hat{a}_i, \quad (1)$$

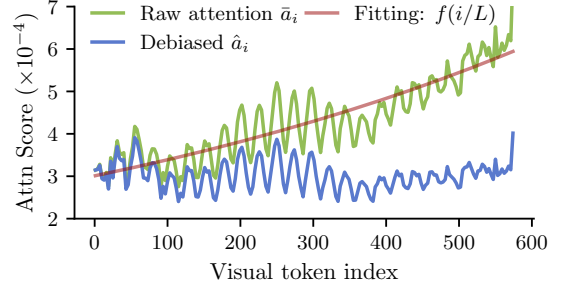


Fig. 2. The average text-to-vision attention scores in LLaVA-v1.5-7B [36] before (left) and after (right) applying our debiasing techniques. The original attention scores exhibit a strong recency bias, favoring visual tokens from lower image regions.

where b_i captures positional bias and \hat{a}_i represents the oracle, content-driven attention. The oracle attention provides a more reliable pruning criterion.

A naive approach is to estimate positional bias b_i by averaging attention scores over large-scale samples. Let a_i^j denote the attention of the j -th image. Since positional bias is content-agnostic, we estimate the bias term as the average attention over N images:

$$b_i \triangleq \bar{a}_i = \frac{1}{N} \sum_{j=1}^N a_i^j, \quad (2)$$

where N is the number of images. The oracle attention is then

$$\hat{a}_i = \frac{a_i}{\bar{a}_i}. \quad (3)$$

However, this direct normalization has two drawbacks. First, \bar{a}_i is often noisy and unstable. Second, it is tied to a fixed number of visual tokens, limiting applicability across models.

To obtain a smooth and length-agnostic positional bias representation, we fit an exponential function to the attention trend. Specifically, we define the parametric curve

$$f_{\mu, \sigma}(x) = \mu \cdot e^{\sigma x}, \quad x \in [0, 1], \quad (4)$$

where μ and σ denote the curve parameters. The parameter σ quantifies the strength of recency bias in the VLM.

We estimate (μ, σ) via least squares:

$$\mu^*, \sigma^* = \arg \min_{\mu, \sigma} \sum_{i=1}^L \sum_{j=1}^N \left\| f_{\mu, \sigma}(i/L) - a_i^j \right\|_2^2,$$

where L is the number of visual tokens. The fitted curve

$$f(x) = \mu^* e^{\sigma^* x} \quad (5)$$

serves as the debiasing denominator, yielding

$$\hat{a}_i = \frac{a_i}{f(i/L)}. \quad (6)$$

This normalization removes content-agnostic recency bias. Fig 2 visualizes the raw average attention \bar{a}_i , the fitted curve $f(i/L)$, and the debiased attention \hat{a}_i .

TABLE I
SUMMARY OF PRUNING CRITERIA, PRUNING GRANULARITY, AND KEY HIGHLIGHTS OF EACH METHOD.

Method	Rank Criterion	Pruning level	Highlights
FastV [9]	Output-to-visual attention	Single-layer	Ranks visual tokens using output-to-visual attention at an early layer, exposing redundancy in deeper visual representations.
PyramidDrop [53]	Output-to-visual attention	Multi-layer	Progressively drops visual tokens across layers, aligning pruning strength with increasing redundancy while balancing efficiency and accuracy.
SparseVLM [63]	Selected text-to-visual attention	Multi-layer	Text-aware, training-free pruning guided by selected language tokens, recycling discarded tokens to preserve fine-grained visual details.
HiMAP [58]	Shallow: text-to-visual attention; Deep: visual-to-visual attention	Multi-layer	Performs hierarchical pruning by modeling depth-wise shifts between cross-modal injection and intra-visual token aggregation.
TokenCarve [49]	Output-to-visual attention	Single-layer	Combines attention ranking with singular value decomposition to select and merge tokens while preserving information content.
iLLaVA [20]	Output-to-visual attention	Multi-layer	Integrates visual token pruning and token merging to reduce redundancy while mitigating information loss under compression.

B. Padding Attention Suppression

Recent studies identify an *attention sink* phenomenon, where LLMs assign disproportionately large attention to semantically meaningless tokens, such as the BOS token or padding tokens in visual inputs. To eliminate this effect, we simply suppress attention to padding tokens by zeroing out their scores:

$$\hat{a}_i = \begin{cases} 0, & \text{if } i \text{ is a padding token,} \\ a_i, & \text{otherwise.} \end{cases} \quad (7)$$

In practice, we first remove recency bias using Eq (6), and then apply padding attention suppression via Eq (7).

C. Discussion

Our method revisits attention-based visual token pruning from a bias-aware perspective, explicitly addressing recency bias and padding-induced attention sinks that distort attention-based ranking. By decoupling content-agnostic positional effects from content-dependent attention, our approach provides a more reliable and interpretable pruning signal. Importantly, the proposed debiasing operations are lightweight, training-free, and can be seamlessly integrated into existing attention-based pruning pipelines.

IV. EXPERIMENTS

In this section, we perform extensive evaluations to answer: **(RQ1)** How effectively does our method improve existing attention-based visual token pruning frameworks across different ranking signals and pruning schemes? **(RQ2)** How robust and general is the approach across model scales (LLaVA-v1.5-7B/13B) and modalities, spanning ten image benchmarks and three video QA benchmarks under constrained token budgets? **(RQ3)** What are the individual contributions of Positional Debiasing and Padding Attention Suppression, and how do recency bias and padding-induced attention sinks manifest in practice?

A. Baseline Pruning Methods

We evaluate our method on six representative attention-based visual token pruning methods. As summarized in Table I, despite differences in pruning granularity and design, these methods rank visual tokens using attention interactions with language or output tokens and prune low-ranked tokens to reduce computational cost.

Specifically, FastV [9] performs attention score rank pruning at a fixed early layer by sorting visual tokens according to output-to-visual attention scores derived from the output token. PyramidDrop [53] extends this strategy to multiple layers, progressively pruning visual tokens across depth using the same output-to-visual attention criterion. HiMAP [58] adopts a hierarchical strategy, where shallow layers prune visual tokens based on language-to-visual attention to capture cross-modal information injection, while deeper layers rely on visual-to-visual attention to model intra-visual aggregation. In contrast, SparseVLM [63] introduces a text-based pruning mechanism by selecting visually relevant language tokens and computing the average attention of these tokens to visual tokens for ranking. TokenCarve [49] combines output-to-visual attention scores with a Singular Value Decomposition (SVD) information contribution metric to select visual tokens for pruning, followed by token merging to preserve attention rank. iLLaVA [20] is based solely on output-to-visual attention scores for pruning and applies token merging to mitigate information loss after pruning.

Together, these methods represent the dominant paradigm of attention-based visual token pruning. In our experiments, we only apply our debiasing techniques to these baselines to examine its effectiveness across different pruning mechanisms and attention sources, and keep all other recipes unchanged.

B. Image Understanding Tasks (RQ1)

Datasets. We evaluate our method on ten representative vision-language benchmarks to comprehensively assess multimodal understanding. VQAv2 [15] focuses on open-ended visual question answering on natural images, while GQA [24] emphasizes compositional reasoning and scene understanding. VizWiz [5] evaluates robustness on real-world images captured

TABLE II

QUANTITATIVE COMPARISON ON TEN VISION–LANGUAGE BENCHMARKS WITH A FIXED BUDGET OF **128** VISUAL TOKENS. RESULTS ARE REPORTED FOR BOTH LLaVA-v1.5-7B AND LLaVA-v1.5-13B BACKBONES. THE ACCURACY (ACC.) IS COMPUTED AS THE AVERAGE OVER ALL BENCHMARKS.

Method	VQAv2	GQA	VizWiz	SQA	TextVQA	POPE	MME	MMB	MMB-CN	MMVet	Acc.
LLaVA-v1.5-7b	78.5	62	50	66.8	58.2	85.9	1510.7	64.3	58.3	31.1	63.1
ToMe [6]	63.0	52.4	50.5	59.6	49.1	62.8	1088.4	53.3	48.8	27.2	52.1
PruMerge+ [44]	74.7	57.8	52.4	67.6	54.3	81.5	1420.5	61.3	54.7	28.7	60.4
VisionZip [55]	75.6	57.6	52.0	68.9	56.8	83.2	1432.4	62.0	56.7	32.6	61.7
FastV[9]	73.2	55.8	51.4	69.1	56.9	72.0	1442.3	63.7	56.6	25.2	59.6
+ Ours	76.6	59.3	51.8	69.1	58.0	83.1	1499.5	63.9	58.0	30.6	62.5
PyramidDrop [53]	75.0	57.0	49.2	69.0	56.1	80.8	1396.5	62.2	56.7	29.3	60.5
+ Ours	76.5	58.9	49.5	68.0	56.7	84.3	1426.8	63.8	56.8	30.5	61.6
SparseVLM[63]	76.3	58.4	50.2	68.7	56.7	85.0	1432.6	64.5	58.3	30.6	62.0
+ Ours	76.7	59.3	50.1	68.5	57.1	85.4	1449.7	64.9	58.8	30.9	62.4
HiMAP[58]	71.0	54.4	49.9	67.5	56.7	75.5	1394.7	62.2	54.7	28.1	59.0
+ Ours	74.8	57.5	51.0	69.1	57.2	80.5	1464.5	63.1	57.2	30.5	61.4
TokenCarve[49]	74.7	57.8	51.0	69.4	58.1	82.4	1482.4	62.6	56.3	28.1	61.5
+ Ours	75.4	58.7	51.5	69.0	57.9	83.6	1489.2	62.7	57.1	28.9	61.9
iLLaVA[20]	71.1	54.8	50.5	68.8	56.4	77.1	1380.5	63.1	56.4	29.3	59.7
+ Ours	74.9	58.0	51.1	68.4	57.2	81.4	1433.4	63.7	57.4	33.3	61.7
LLaVA-v1.5-13B	80.0	63.3	53.6	71.6	61.3	86.0	1531.3	67.7	63.6	36.1	66.0
FastV [9]	76.5	59.1	54.5	74.1	59.6	81.1	1473.3	66.8	62.4	34.9	64.3
+ Ours	78.2	60.9	55.8	73.9	60.0	83.7	1503.7	67.4	63.1	34.0	65.2
PyramidDrop [53]	76.7	58.6	53.9	72.5	58.8	84.6	1489.4	65.6	61.6	34.6	64.1
+ Ours	77.5	60.0	55.0	72.7	59.1	85.6	1492.4	67.2	61.7	34.9	64.8
SparseVLM[63]	77.1	58.6	55.1	74.2	59.1	84.4	1495.1	68.3	62.9	37.9	65.2
+ Ours	77.4	58.8	55.4	74.2	59.2	85.0	1494.2	68.4	62.9	37.0	65.3
HiMAP[58]	75.2	58.2	52.5	72.5	58.5	79.5	1459.6	66.1	61.8	34.3	63.2
+ Ours	77.0	59.4	54.3	72.1	59.0	81.5	1488.4	67.0	62.3	35.4	64.2
TokenCarve[49]	77.6	61.8	54.0	73.4	60.6	87.3	1500.5	67.7	61.8	34.3	65.4
+ Ours	78.6	62.0	55.3	73.3	60.4	87.6	1523.7	67.4	62.3	35.0	65.8
iLLaVA[20]	76.1	59.0	53.8	73.9	59.2	80.6	1462.3	66.1	62.5	34.8	63.9
+ Ours	77.8	60.8	54.5	73.7	59.7	82.9	1473.7	66.6	63.3	35.7	64.9

by blind users. ScienceQA-Image [39] targets science-oriented multimodal reasoning, and TextVQA [46] evaluates question answering over text-rich images. POPE [33] measures robustness against hallucinated yet plausible answers. MME [13], MMBench, MMBench-CN [38], and MM-Vet [59] provide broad evaluations of perception, reasoning, and multimodal dialogue across both English and Chinese settings.

Implementation Details. We evaluate our method on both attention-based and non-attention-based visual token pruning approaches, comparing against representative non-attention-based methods including ToMe [6], PruMerge+ [44], and VisionZip [55]. In addition, our method is applied as a plug-and-play enhancement to six attention-based pruning frameworks, namely FastV [9], PyramidDrop [53], SparseVLM [63], HiMAP [58], TokenCarve [49], and iLLaVA [20], to assess its generality across different pruning strategies. All experiments are conducted on LLaVA-v1.5-7B and LLaVA-v1.5-13B [36], both built upon the Vicuna language model and the CLIP [41] visual encoder, and are performed during inference on a single NVIDIA A100 GPU with 80 GB memory.

Quantitative Results. Table II reports quantitative results on ten vision–language benchmarks with a fixed budget of

128 visual tokens. Our method consistently improves all attention-based pruning baselines on both LLaVA-v1.5-7B and LLaVA-v1.5-13B. On LLaVA-v1.5-7B, applying our method to FastV increases the overall accuracy from 59.6 to 62.5, while integrating it with PyramidDrop and HiMAP yields gains of +1.1 and +2.4 points, respectively. On LLaVA-v1.5-13B, our method further boosts FastV from 64.3 to 65.2 and TokenCarve from 65.4 to 65.8. These results demonstrate that debiasing attention-based ranking directly translates into more effective visual token pruning.

Qualitative Results Figure 3 presents qualitative comparisons of visual token pruning results for FastV [9], PyramidDrop [53], SparseVLM [63], and HiMAP [58]. Under the original pruning strategies, many retained visual tokens are biased toward padded regions or the bottom of the image, indicating that attention-based pruning can favor positionally late or non-informative tokens. In contrast, our method suppresses such biased retention and preserves fine-grained, semantically relevant visual information. For example, in the third row, SparseVLM retains padded tokens near the image bottom while discarding patches corresponding to key digits (i.e., digits ‘2’, ‘3’, and ‘4’) on the ruler, leading to an incorrect



Fig. 3. Qualitative visualization of visual token pruning results for FastV, PyramidDrop, SparseVLM, and HiMAP. Retained visual tokens are overlaid on the input images for each method before and after applying our approach. Existing pruning methods tend to preserve tokens in padded or bottom regions while discarding fine-grained, question-relevant patches. In contrast, our method suppresses the retention of padded regions and consistently preserves semantically important visual tokens, leading to more accurate predictions.

prediction. After applying our method, padded regions are removed and the relevant digit patches are preserved, enabling correct recognition.

1) *Token Selection under Different Image Ratios*: We analyze how image aspect ratio affects visual token selection using the TextVQA [46] dataset, grouping images into square, portrait, and landscape categories. Figure 4 reveals that FastV [9] exhibits strong positional bias across all settings, favoring visual tokens located in the lower regions for square images and frequently retaining padded boundary regions for portrait and landscape images, regardless of semantic relevance. In contrast, our method produces substantially more uniform spatial selection patterns, effectively mitigating both recency bias and padding-induced attention bias across all aspect ratios.

C. Video Understanding (RQ2)

Datasets. To further evaluate the effectiveness of our method in temporal multimodal understanding, we conduct experiments on three widely used video–language benchmarks: TGIF-QA [25], MSVD-QA [54], and MSR-VTT-QA [54]. These benchmarks cover diverse video question answering scenarios that require joint reasoning over visual content, temporal dynamics, and language queries. Following prior works [35], [60], [63], we report both accuracy and GPT-based evaluation scores for comprehensive assessment.

Implementation Details. We integrate our method into the Video-LLaVA framework [35], which extends LLaVA to the video domain by encoding video frames into visual tokens for multimodal reasoning. In our experiments, the original sequence of 2048 video tokens is pruned to 512 tokens to evaluate the effectiveness of visual token reduction in video

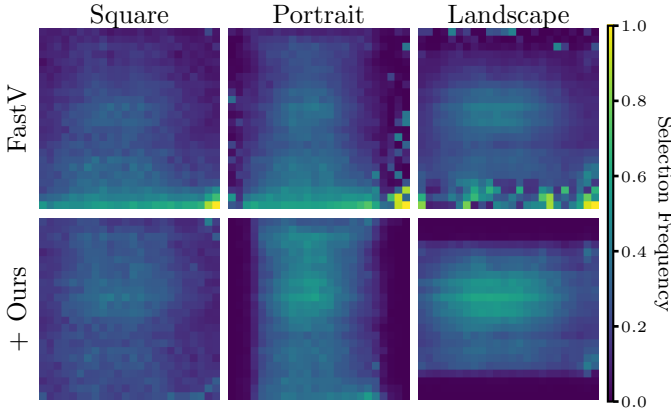


Fig. 4. Visualization of visual token selection frequency across different image aspect ratios (square, portrait, and landscape) on TextVQA. Brighter regions denote higher token selection frequency. FastV shows strong bias toward padded or lower image regions in portrait and landscape inputs, where outlier tokens are selected disproportionately often, whereas our method yields a more balanced and spatially uniform selection pattern.

TABLE III
RESULTS ON VIDEO QUESTION ANSWERING BENCHMARKS UNDER A FIXED BUDGET OF 512 VIDEO TOKENS.

Method	MSRVTT [54]		MSVD [54]		TGIF [25]		Avg.
	Acc.	Score	Acc.	Score	Acc.	Score	
V-LLaVA [35]	58.3	3.50	70.1	3.90	47.1	3.40	58.5 4.60
FastV [9]	56.1	3.43	70.3	3.87	45.4	3.33	57.3 3.54
+ Ours	56.5	3.45	70.6	3.90	46.6	3.39	57.9 3.58
PDrop [53]	57.1	3.46	70.1	3.89	46.3	3.35	57.8 3.57
+ Ours	57.3	3.47	70.0	3.87	46.5	3.37	57.9 3.57
SparseVLM [63]	56.9	3.44	70.0	3.88	46.0	3.34	57.6 3.55
+ Ours	57.4	3.48	70.5	3.91	46.7	3.38	58.2 3.59
HiMAP [58]	57.0	3.45	70.2	3.89	47.2	3.36	58.1 3.57
+ Ours	57.6	3.49	70.7	3.92	46.9	3.33	58.4 3.58

understanding. Our method is applied as a plug-and-play module on top of existing attention-based pruning baselines, including FastV [9], PyramidDrop [53], SparseVLM [63], and HiMAP [58], without additional training or architectural modifications.

Quantitative Results. Table III reports results on three video QA benchmarks with a fixed budget of 512 video tokens. Our method consistently improves all attention-based pruning baselines. For FastV, the average accuracy increases from 57.3% to 57.9% and the GPT score from 3.54 to 3.58. For SparseVLM, accuracy improves from 57.6% to 58.2% and the GPT score from 3.55 to 3.59. These results confirm the effectiveness of our method under a constrained video token budget.

D. Ablation Study (RQ3)

1) *Effect of Debiasing Techniques* : Our method comprises two key components to mitigate attention bias in visual token pruning: (1) Positional Debiasing and (2) Padding Attention Suppression.

TABLE IV

ABLATION OF THE PROPOSED DEBIASING COMPONENTS TOP OF FASTV AND PYRAMIDDROP UNDER THE SAME RETAINED VISUAL TOKENS 128. PD: POSITIONAL DEBIASING; PAS: PADDING ATTENTION SUPPRESSION.

Method	PD	PAS	VQAv2	GQA	TextVQA	Avg.
FastV [9]	✗	✗	73.2	55.8	56.9	62.0
	✓	✗	76.0	58.3	57.7	64.0
	✗	✓	76.3	58.8	57.6	64.2
	✓	✓	76.6	59.3	58.0	64.6
PyramidDrop [53]	✗	✗	75.0	57.0	56.1	62.7
	✓	✗	76.1	58.4	56.2	63.6
	✗	✓	76.2	58.7	56.4	63.8
	✓	✓	76.5	58.9	56.7	64.0

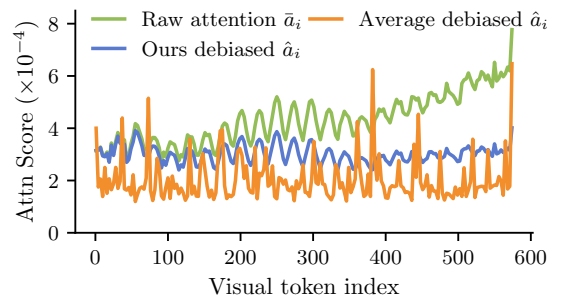


Fig. 5. Text-to-vision attention trends in three settings: original attention, the average attention debias using Eq (2), and the fitted exponential trend debiasing using Eq (5). Directly using the average attention leaves clear positional bias, while exponential fitting yields a smoother, position-agnostic attention trend.

Table IV reports ablation results of Positional Debiasing (PD) and Padding Attention Suppression (PAS) on two representative attention-based pruning methods: FastV [9] (single-layer pruning) and PyramidDrop [53] (multi-layer pruning). For FastV, applying Positional Debiasing or Padding Attention Suppression individually improves the average accuracy from 62.0 to 64.0 and 64.2, respectively, while combining both yields the best performance at 64.6. A similar trend is observed for PyramidDrop, where each component consistently improves performance and their combination achieves the strongest results. These results demonstrate that Positional Debiasing and Padding Attention Suppression address complementary sources of bias, and their joint application leads to the most stable and effective gains across benchmarks.

2) *Modeling the Positional Bias Trend* : As described in the methodology, we consider two strategies for modeling the positional bias trend: (i) Eq (2), which directly uses the average attention and is often noisy and unstable, and (ii) Eq (5), which models the trend using a smooth exponential function. This ablation compares these two modeling choices to validate our design. Figure 5 visualizes the text-to-vision attention trends in three settings: original attention, debiasing using the average attention, and debiasing with the fitted exponential trend, while Table V (above) reports the corresponding quantitative results in benchmarks. The results show that directly using the average attention leads to noisy and suboptimal debiasing, whereas the exponential trend provides a smoother and more reliable bias estimation, resulting better performance.

TABLE V

COMPARISON OF DIFFERENT POSITIONAL BIAS MITIGATION TECHNIQUES. TOP: EXPONENTIAL TREND FITTING (EQ (5)) CONSISTENTLY OUTPERFORMS DIRECT USE OF AVERAGE ATTENTION (EQ (2)). BOTTOM: COMPARING WITH [11], OUR METHOD ACHIEVES CONSISTENTLY SUPERIOR PERFORMANCE ACROSS ALL MODELS AND BENCHMARKS.

Method	VQAv2	GQA	VizWiz	SQA	TextVQA	POPE	MME	MMB	MMB-CN	MMVet	Avg.
FastV [9]	73.2	55.8	51.4	69.1	56.9	72.0	1442.3	63.7	56.6	25.2	59.6
FastV + Eq (2)	72.2	55.6	50.8	68.2	56.8	76.7	1383.5	62.9	55.8	30.0	59.8
FastV + Eq (5)	76.0	58.3	51.4	69.4	57.7	77.6	1498.4	63.8	57.4	30.3	61.7
FastV+ [11]	69.7	54.2	51.2	70.2	57.9	73.9	1329.8	59.6	50.9	30.0	58.4
FastV + Ours	76.6	59.3	51.8	69.1	58.0	83.1	1499.5	63.9	58.0	30.6	62.5

TABLE VI

PERFORMANCE OF DIFFERENT RETAINING TOKENS ON TEXTVQA ACCURACY, WITH PRUNING APPLIED AT LAYER 2.

Retain	FastV		PyramidDrop		HiMAP	
	Base	+Ours	Base	+Ours	Base	+Ours
64	55.1	57.1	55.3	55.9	55.6	56.0
96	56.3	57.5	55.7	56.2	56.2	56.8
128	56.9	58.0	56.1	56.7	56.7	57.2
192	57.3	57.9	56.5	57.5	57.0	57.5
256	57.5	58.1	57.1	57.8	57.4	57.9

TABLE VII

PERFORMANCE OF PRUNING DIFFERENT LAYERS AT DIFFERENT DEPTHS ON TEXTVQA, WITH THE RETAIN-TOKEN BUDGET FIXED AT 128.

Layer	FastV		PyramidDrop		HiMAP	
	Base	+Ours	Base	+Ours	Base	+Ours
1	55.6	56.9	55.0	55.5	55.4	56.1
2	56.9	58.0	56.1	56.7	56.7	57.2
4	57.3	57.9	56.9	57.4	57.1	57.4
8	57.5	58.1	57.6	57.8	57.3	57.6
16	58.0	58.1	58.0	58.1	57.5	57.9

3) *Number of Retaining Tokens and Pruning Layers* : We analyze the impact of the number of retaining tokens and pruning layers on TextVQA [46] using LLaVA-v1.5-7B [36]. Table VI reports the results under varying numbers of retained visual tokens with the pruning layer fixed at layer 2 for FastV [9], PyramidDrop [53], and HiMAP [58]. Across all three pruning methods, our approach consistently outperforms the corresponding baselines under different retain token budgets. Notably, the performance gains become more pronounced as the retain budget decreases, indicating that the proposed method is particularly effective under more aggressive token pruning.

Table VII further examines the effect of applying pruning at different decoder layers with the retain token budget fixed at 128. For FastV, PyramidDrop, and HiMAP, our method provides stable and consistent improvements across a wide range of pruning layers. Although pruning at very early layers generally leads to larger performance degradation for all methods, our approach effectively mitigates this effect and achieves higher accuracy at each pruning layer. Overall, these results demonstrate that the proposed method is robust to both the retain token budget and the pruning layer, serving as a general enhancement for attention-based visual token pruning

strategies.

E. Attention Bias in Visual Token Pruning

We analyze systematic attention biases in attention-based visual token pruning. In particular, we first examine recency bias as a fundamental positional bias in visual token ranking, and then analyze how padding further amplifies this bias through attention sink effects.

1) *Recency Bias in Visual Token Selection*: We first analyze recency bias by visualizing the selection frequency along visual token indices. As shown in Figure 6, the selection frequency along visual token indices is visualized for FastV [9], SparseVLM [63], and HiMAP [58] to examine recency bias in attention-based visual token pruning.

Although these methods adopt different ranking criteria (see Table I), they all exhibit a clear preference for tokens with larger indices, i.e., tokens appearing later in the visual token sequence. This consistent upward trend indicates that recency bias is a common and systematic issue across attention-based pruning strategies, motivating the following quantitative analysis and investigation into its underlying causes.

2) *Quantitative Analysis of Recency Bias* : To quantitatively measure recency bias in attention-based visual token pruning, we model positional trends in both attention scores and pruning results using exponential fitting. For each benchmark and pruning method, we compute two curves along the visual token index: (i) the dataset-averaged attention score

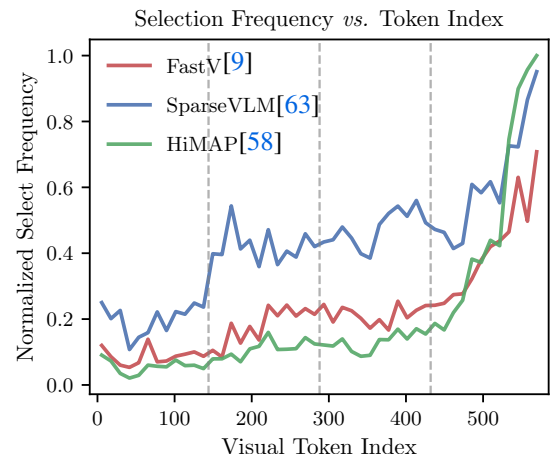


Fig. 6. Selection frequency over visual token indices for FastV, SparseVLM, and HiMAP, highlighting recency bias in visual token pruning.

TABLE VIII

QUANTIFYING RECENTY BIAS VIA BIAS STRENGTHS. WE REPORT THE BIAS STRENGTHS OF THE AVERAGED ATTENTION SCORES (σ_{attn}) AND TOKEN SELECTION FREQUENCIES (σ_{freq}), WHERE LARGER VALUES INDICATE STRONGER RECENTY BIAS.

Method	VQAv2		SQA		POPE		MME	
	$ \sigma_{\text{attn}} \downarrow \sigma_{\text{freq}} \downarrow $							
FastV [9]	0.91	2.56	0.70	1.55	0.96	2.73	0.80	2.07
+ Ours	-0.01	-0.10	-0.14	-0.47	0.07	0.12	-0.03	-0.07
PDrop [53]	1.29	2.48	1.25	1.60	1.45	2.51	1.07	2.06
+ Ours	-0.23	0.37	-0.25	-0.45	-0.10	0.26	-0.13	0.34
SparseVLM [63]	1.37	2.00	1.44	1.42	1.52	2.07	1.12	1.66
+ Ours	-0.21	0.21	-0.32	-0.28	-0.31	0.36	-0.28	0.13
HiMAP [58]	0.99	2.90	0.80	2.00	1.00	3.06	0.94	2.39
+ Ours	-0.34	0.31	-0.16	-0.50	-0.34	-0.28	-0.35	0.21

TABLE IX

QUANTITATIVE COMPARISON OF DIFFERENT PADDING MODES USING FASTV ON VQAV2, GQA, AND TEXTVQA. “REMOVE” DENOTES THE PROPOSED PADDING-AWARE FILTERING.

Method	Pad Mode	VQAv2	GQA	TextVQA	Avg.
FastV [9]	Mean	73.2	55.8	56.9	62.0
	Constant	73.4	55.3	57.3	62.0
	Random	74.1	55.5	57.0	62.2
	Mirror	73.9	56.0	57.0	62.3
+ Ours	Remove	76.3	58.8	57.6	64.2

curve and (ii) the token selection frequency induced by top- K pruning. Each curve is fitted with the exponential function in Eq (4), yielding the bias strengths σ_{attn} and σ_{freq} , respectively, where larger values indicate stronger recency bias.

Table VIII reports these rates across four benchmarks and four representative pruning methods. All baseline methods exhibit clear recency bias, with consistently positive σ_{attn} values, indicating monotonically increasing attention toward later tokens. More critically, this bias is significantly amplified during pruning, as reflected by much larger σ_{freq} , explaining the systematic over-retention of visually uninformative tail tokens. After applying our method, both bias strengths are sharply reduced to near zero across all settings, demonstrating effective suppression of recency bias and preventing its amplification in token ranking and selection.

3) *RoPE and Recency Bias* : A recent work [11] attributes recency bias to the long-term decay property of Rotary Positional Embedding (RoPE) [47] and proposes removing RoPE during attention-score computation for token ranking. We reproduce this RoPE-free scoring strategy within the FastV [9] framework. As shown in Table V (below), removing RoPE does not yield consistent improvements. In contrast, our method consistently improves performance across all benchmarks, indicating that correcting biased attention signals is more effective than disabling positional encoding.

4) *Padding-Induced Attention Sink*: We analyze why visual tokens originating from padded regions are disproportionately retained during attention-based pruning. Motivated by prior studies on visual attention sinks [27], we hypothesize that padding regions are particularly prone to inducing sink behavior. In LLaVA-v1.5-7B [36], padded image regions are

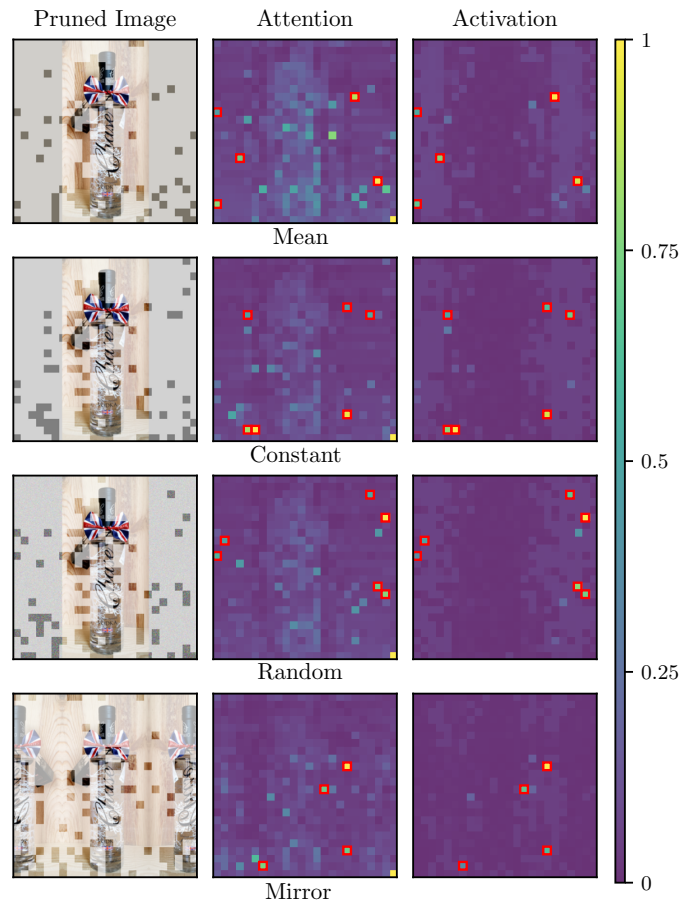


Fig. 7. Attention sink visualization under different padding modes: (a) mean padding, (b) constant padding, (c) random padding, and (d) mirror padding. Uninformative padding induces attention sinks in padded regions, whereas mirror padding shifts attention toward meaningful background content.

semantically meaningless, but the corresponding visual tokens nonetheless show abnormally large activations in certain hidden-state dimensions. These extreme activations propagate into attention computation, producing inflated attention scores that bias the pruning criterion toward retaining padded tokens.

Figure 7 (Mean) qualitatively illustrates this effect. From left to right, we visualize the retained visual tokens mapped to the input image, the attention scores used for pruning, and the hidden-state activations at the pruning layer. Highlighted regions show that padded tokens are consistently preserved and simultaneously exhibit high attention scores and strong activations, providing direct evidence that padding-induced attention sinks distort visual token selection.

5) *Effect of Different Padding Modes* : We analyze the impact of different padding modes on attention-based visual token pruning. Figure 7 compares four padding strategies: *Mean*, *Constant*, *Random*, and *Mirror*. For padding modes that introduce no semantic content (*Mean*, *Constant*, and *Random*), attention sinks consistently appear in padded regions, leading to abnormally high activations and attention scores that cause padded tokens to be erroneously retained. In contrast, when padding contains meaningful visual structure (*Mirror*), attention sinks shift toward structured background regions rather than padded borders, consistent with prior observations [27].

Quantitative results in Table IX show that different padding values lead to similar performance across benchmarks, indicating that padding-induced bias cannot be eliminated through padding design alone. While mirror padding provides only limited improvements, our padding-aware filtering explicitly removes padded tokens and yields substantially larger gains, increasing the average accuracy from 62.0 to 64.2. These findings confirm that the primary source of biased visual token pruning lies in padding-induced attention sinks rather than in the specific choice of padding modes.

V. CONCLUSION

In this work, we revisit visual token pruning in vision-language models through the lens of attention bias. We show that commonly used attention-based pruning signals are systematically distorted by two intrinsic effects inherited from large language models: recency bias, which over-favors later visual tokens, and attention sink behavior, which assigns inflated scores to semantically empty padding tokens. To restore attention as a more reliable pruning criterion, we propose two lightweight, training-free debiasing techniques—positional debiasing and padding-aware attention suppression—that can be plugged into existing pruning frameworks with only a few lines of code. Extensive experiments on ten image benchmarks and three video benchmarks demonstrate consistent gains across six representative attention-based pruning methods under fixed token budgets.

Our method has limitations. Padding-aware suppression only applies to encoders that explicitly introduce padding; padding-free or differently tokenized architectures cannot directly benefit from this component. Moreover, our approach mitigates biased attention signals during inference rather than fundamentally eliminating their root causes. Recency bias and attention sinks stem from the underlying modeling and optimization properties of large language models, and correcting attention scores does not fully resolve potential biases in representations or dynamics. Future work may explore more principled, architecture-agnostic debiasing and training-time strategies to address attention bias more fundamentally.

ACKNOWLEDGEMENTS

This work was partially supported by the National Natural Science Foundation of China (62372284, 62476143), the National Key Laboratory of Science and Technology on Space-Born Intelligent Information Processing (TJ-02-22-01), and the Pioneer R&D Program of Zhejiang Province (2024C01024). We thank Professor Liang Zheng from Australian National University for his valuable suggestions on this work.

REFERENCES

- [1] Saeed Ranjbar Alvar, Gursimran Singh, Mohammad Akbari, and Yong Zhang. Divprune: Diversity-based visual token pruning for large multimodal models. In *Proceedings of the Computer Vision and Pattern Recognition Conference*, pages 9392–9401, 2025.
- [2] Kazi Hasan Ibn Arif, JinYi Yoon, Dimitrios S Nikolopoulos, Hans Vandierendonck, Deepu John, and Bo Ji. Hired: Attention-guided token dropping for efficient inference of high-resolution vision-language models. In *Proceedings of the AAAI Conference on Artificial Intelligence*, volume 39, pages 1773–1781, 2025.
- [3] Shuai Bai, Yuxuan Cai, Ruizhe Chen, Keqin Chen, Xionghui Chen, Zesen Cheng, Lianghao Deng, Wei Ding, Chang Gao, Chunjiang Ge, Wenbin Ge, Zhifang Guo, Qidong Huang, Jie Huang, Fei Huang, Binyuan Hui, Shutong Jiang, Zhaohai Li, Mingsheng Li, Mei Li, Kaixin Li, Zicheng Lin, Junyang Lin, Xuejing Liu, Jiawei Liu, Chenglong Liu, Yang Liu, Dayiheng Liu, Shixuan Liu, Dunjie Lu, Ruilin Luo, Chenxu Lv, Rui Men, Lingchen Meng, Xuancheng Ren, Xingzhang Ren, Sibo Song, Yuchong Sun, Jun Tang, Jianhong Tu, Jianqiang Wan, Peng Wang, Pengfei Wang, Qiyue Wang, Yuxuan Wang, Tianbao Xie, Yiheng Xu, Haiyang Xu, Jin Xu, Zhibo Yang, Mingkun Yang, Jianxin Yang, An Yang, Bowen Yu, Fei Zhang, Hang Zhang, Xi Zhang, Bo Zheng, Humen Zhong, Jingren Zhou, Fan Zhou, Jing Zhou, Yuanzhi Zhu, and Ke Zhu. Qwen3-v1 technical report. *arXiv preprint arXiv:2511.21631*, 2025.
- [4] Federico Barbero, Alvaro Arroyo, Xiangming Gu, Christos Perivolopoulos, Petar Veličković, Razvan Pascanu, and Michael M. Bronstein. Why do LLMs attend to the first token? In *Second Conference on Language Modeling*, 2025.
- [5] Jeffrey P Bigham, Chandrika Jayant, Hanjie Ji, Greg Little, Andrew Miller, Robert C Miller, Robin Miller, Aubrey Tatarowicz, Brandyn White, Samual White, et al. Vizwiz: nearly real-time answers to visual questions. In *Proceedings of the 23rd annual ACM symposium on User interface software and technology*, pages 333–342, 2010.
- [6] Daniel Bolya, Cheng-Yang Fu, Xiaoliang Dai, Peizhao Zhang, Christoph Feichtenhofer, and Judy Hoffman. Token merging: Your ViT but faster. In *International Conference on Learning Representations*, 2023.
- [7] Mu Cai, Jianwei Yang, Jianfeng Gao, and Yong Jae Lee. Matryoshka multimodal models. In *The Thirteenth International Conference on Learning Representations*, 2025.
- [8] Jieneng Chen, Luoxin Ye, Ju He, Zhao-Yang Wang, Daniel Khashabi, and Alan Yuille. Efficient large multi-modal models via visual context compression. *Advances in Neural Information Processing Systems*, 37:73986–74007, 2024.
- [9] Liang Chen, Haozhe Zhao, Tianyu Liu, Shuai Bai, Junyang Lin, Chang Zhou, and Baobao Chang. An image is worth 1/2 tokens after layer 2: Plug-and-play inference acceleration for large vision-language models. In *European Conference on Computer Vision*, pages 19–35. Springer, 2024.
- [10] Zihang Dai, Guokun Lai, Yiming Yang, and Quoc Le. Funnel-transformer: Filtering out sequential redundancy for efficient language processing. *Advances in neural information processing systems*, 33:4271–4282, 2020.
- [11] Mark Endo, Xiaohan Wang, and Serena Yeung-Levy. Feather the throttle: Revisiting visual token pruning for vision-language model acceleration. In *Proceedings of the IEEE/CVF International Conference on Computer Vision (ICCV)*, pages 22826–22835, October 2025.
- [12] Qihua Feng, Peiya Li, Zhixun Lu, Chaozhuo Li, Zefan Wang, Zhiqian Liu, Chunhui Duan, Feiran Huang, Jian Weng, and Philip S Yu. Evit: Privacy-preserving image retrieval via encrypted vision transformer in cloud computing. *IEEE Transactions on Circuits and Systems for Video Technology*, 34(8):7467–7483, 2024.
- [13] Chaoyou Fu, Peixian Chen, Yunhang Shen, Yulei Qin, Mengdan Zhang, Xu Lin, Jinrui Yang, Xiawu Zheng, Ke Li, Xing Sun, Yunsheng Wu, Rongrong Ji, Caifeng Shan, and Ran He. MME: A comprehensive evaluation benchmark for multimodal large language models. In *The Thirty-ninth Annual Conference on Neural Information Processing Systems Datasets and Benchmarks Track*, 2025.
- [14] Yash Goyal, Tejas Khot, Douglas Summers-Stay, Dhruv Batra, and Devi Parikh. Making the v in vqa matter: Elevating the role of image understanding in visual question answering. In *2017 IEEE Conference on Computer Vision and Pattern Recognition (CVPR)*, pages 6325–6334, 2017.
- [15] Yash Goyal, Tejas Khot, Douglas Summers-Stay, Dhruv Batra, and Devi Parikh. Making the v in vqa matter: Elevating the role of image understanding in visual question answering. In *Proceedings of the IEEE conference on computer vision and pattern recognition*, pages 6904–6913, 2017.
- [16] Xiangming Gu, Tianyu Pang, Chao Du, Qian Liu, Fengzhuo Zhang, Cunxiao Du, Ye Wang, and Min Lin. When attention sink emerges in language models: An empirical view. In *The Thirteenth International Conference on Learning Representations*, 2025.
- [17] Xiaobo Guo and Soroush Vosoughi. Serial position effects of large language models. In *Findings of the Association for Computational Linguistics: ACL 2025*, pages 927–953, 2025.
- [18] Xiangyu Hong, Che Jiang, Biqing Qi, Fandong Meng, Mo Yu, Bowen Zhou, and Jie Zhou. On the token distance modeling ability of higher rope attention dimension. In *Findings of the 2024 Conference on*

Empirical Methods in Natural Language Processing (EMNLP), pages 5877–5888, 2024.

[19] Marc W Howard and Michael J Kahana. A distributed representation of temporal context. *Journal of mathematical psychology*, 46(3):269–299, 2002.

[20] Lianyu Hu, Fanhua Shang, Liang Wan, and Wei Feng. illava: An image is worth fewer than 1/3 input tokens in large multimodal models. *arXiv preprint arXiv:2412.06263*, 2024.

[21] Wenbo Hu, Zi-Yi Dou, Liunian Harold Li, Amita Kamath, Nanyun Peng, and Kai-Wei Chang. Matryoshka query transformer for large vision-language models. In *Proceedings of the 38th International Conference on Neural Information Processing Systems*, pages 50168–50188, 2024.

[22] Kai Huang, Hao Zou, Ye Xi, BoChen Wang, Zhen Xie, and Liang Yu. Ivtp: Instruction-guided visual token pruning for large vision-language models. In *European Conference on Computer Vision*, pages 214–230. Springer, 2024.

[23] Wexuan Huang, Zijie Zhai, Yunhang Shen, Shaosheng Cao, Fei Zhao, Xiangfeng Xu, Zheyu Ye, and Shaohui Lin. Dynamic-LLaVA: Efficient multimodal large language models via dynamic vision-language context sparsification. In *The Thirteenth International Conference on Learning Representations*, 2025.

[24] Drew A Hudson and Christopher D Manning. Gqa: A new dataset for real-world visual reasoning and compositional question answering. In *Proceedings of the IEEE/CVF conference on computer vision and pattern recognition*, pages 6700–6709, 2019.

[25] Yunseok Jang, Yale Song, Youngjae Yu, Youngjin Kim, and Gunhee Kim. Tgif-qa: Toward spatio-temporal reasoning in visual question answering. In *Proceedings of the IEEE conference on computer vision and pattern recognition*, pages 2758–2766, 2017.

[26] Yutao Jiang, Qiong Wu, Wenhao Lin, Wei Yu, and Yiyi Zhou. What kind of visual tokens do we need? training-free visual token pruning for multi-modal large language models from the perspective of graph. In *Proceedings of the AAAI Conference on Artificial Intelligence*, volume 39, pages 4075–4083, 2025.

[27] Seil Kang, Jinyeong Kim, Junhyeok Kim, and Seong Jae Hwang. See what you are told: Visual attention sink in large multimodal models. In *The Thirteenth International Conference on Learning Representations*, 2025.

[28] Zhenglun Kong, Peiyan Dong, Xiaolong Ma, Xin Meng, Wei Niu, Mengshu Sun, Xuan Shen, Geng Yuan, Bin Ren, Hao Tang, et al. Spvit: Enabling faster vision transformers via latency-aware soft token pruning. In *European conference on computer vision*, pages 620–640. Springer, 2022.

[29] Xin Lai, Zhuotao Tian, Yukang Chen, Yanwei Li, Yuhui Yuan, Shu Liu, and Jiaya Jia. Lisa: Reasoning segmentation via large language model. In *2024 IEEE/CVF Conference on Computer Vision and Pattern Recognition (CVPR)*, pages 9579–9589, 2024.

[30] Junnan Li, Dongxu Li, Caiming Xiong, and Steven Hoi. Blip: Bootstrapping language-image pre-training for unified vision-language understanding and generation. In *ICML*, 2022.

[31] Wentong Li, Yuqian Yuan, Jian Liu, Dongqi Tang, Song Wang, Jie Qin, Jian Zhu, and Lei Zhang. Tokenpacker: Efficient visual projector for multimodal llm. *International Journal of Computer Vision*, pages 1–19, 2025.

[32] Yanwei Li, Chengyao Wang, and Jiaya Jia. Llama-vid: An image is worth 2 tokens in large language models. In *European Conference on Computer Vision*, pages 323–340. Springer, 2024.

[33] Yifan Li, Yifan Du, Kun Zhou, Jinpeng Wang, Wayne Xin Zhao, and Ji-Rong Wen. Evaluating object hallucination in large vision-language models. In *Proceedings of the 2023 Conference on Empirical Methods in Natural Language Processing*, pages 292–305, 2023.

[34] Zhang Li, Biao Yang, Qiang Liu, Shuo Zhang, Zhiyin Ma, Liang Yin, Linger Deng, Yabo Sun, Yuliang Liu, and Xiang Bai. Lira: Inferring segmentation in large multi-modal models with local interleaved region assistance. In *Proceedings of the IEEE/CVF International Conference on Computer Vision (ICCV)*, pages 24056–24067, October 2025.

[35] Bin Lin, Yang Ye, Bin Zhu, Jiaxi Cui, Munan Ning, Peng Jin, and Li Yuan. Video-llava: Learning united visual representation by alignment before projection. In *Proceedings of the 2024 Conference on Empirical Methods in Natural Language Processing*, pages 5971–5984, 2024.

[36] Haotian Liu, Chunyuan Li, Qingyang Wu, and Yong Jae Lee. Visual instruction tuning. *Advances in neural information processing systems*, 36:34892–34916, 2023.

[37] Nelson F Liu, Kevin Lin, John Hewitt, Ashwin Paranjape, Michele Bevilacqua, Fabio Petroni, and Percy Liang. Lost in the middle: How language models use long contexts. *Transactions of the Association for Computational Linguistics*, 12:157–173, 2024.

[38] Yuan Liu, Haodong Duan, Yuanhan Zhang, Bo Li, Songyang Zhang, Wangbo Zhao, Yike Yuan, Jiaqi Wang, Conghui He, Ziwei Liu, et al. Mmbench: Is your multi-modal model an all-around player? In *European conference on computer vision*, pages 216–233. Springer, 2024.

[39] Pan Lu, Swaroop Mishra, Tanglin Xia, Liang Qiu, Kai-Wei Chang, Song-Chun Zhu, Oyvind Tafjord, Peter Clark, and Ashwin Kalyan. Learn to explain: Multimodal reasoning via thought chains for science question answering. *Advances in Neural Information Processing Systems*, 35:2507–2521, 2022.

[40] Bennet B Murdock Jr. The serial position effect of free recall. *Journal of experimental psychology*, 64(5):482, 1962.

[41] Alec Radford, Jong Wook Kim, Chris Hallacy, Aditya Ramesh, Gabriel Goh, Sandhini Agarwal, Girish Sastry, Amanda Askell, Pamela Mishkin, Jack Clark, Gretchen Krueger, and Ilya Sutskever. Learning transferable visual models from natural language supervision. In Marina Meila and Tong Zhang, editors, *Proceedings of the 38th International Conference on Machine Learning*, volume 139 of *Proceedings of Machine Learning Research*, pages 8748–8763. PMLR, 18–24 Jul 2021.

[42] Jack W. Rae, Anna Potapenko, Siddhant M. Jayakumar, Chloe Hillier, and Timothy P. Lillicrap. Compressive transformers for long-range sequence modelling. In *International Conference on Learning Representations*, 2020.

[43] Yongming Rao, Wenliang Zhao, Benlin Liu, Jiwen Lu, Jie Zhou, and Cho-Jui Hsieh. Dynamicvlt: Efficient vision transformers with dynamic token sparsification. In *Advances in Neural Information Processing Systems (NeurIPS)*, 2021.

[44] Yuzhang Shang, Mu Cai, Bingxin Xu, Yong Jae Lee, and Yan Yan. Llava-prumerge: Adaptive token reduction for efficient large multimodal models. In *Proceedings of the IEEE/CVF International Conference on Computer Vision*, pages 22857–22867, 2025.

[45] Amanpreet Singh, Vivek Natarajan, Meet Shah, Yu Jiang, Xinlei Chen, Dhruv Batra, Devi Parikh, and Marcus Rohrbach. Towards vqa models that can read. In *2019 IEEE/CVF Conference on Computer Vision and Pattern Recognition (CVPR)*, pages 8309–8318, 2019.

[46] Amanpreet Singh, Vivek Natarajan, Meet Shah, Yu Jiang, Xinlei Chen, Dhruv Batra, Devi Parikh, and Marcus Rohrbach. Towards vqa models that can read. In *Proceedings of the IEEE/CVF conference on computer vision and pattern recognition*, pages 8317–8326, 2019.

[47] Jianlin Su, Murtadha Ahmed, Yu Lu, Shengfeng Pan, Wen Bo, and Yunfeng Liu. Roformer: Enhanced transformer with rotary position embedding. *Neurocomputing*, 568:127063, 2024.

[48] Jingyu Sun, Yizheng Sun, Riza Theresa Batista-Navarro, and Chenghua Lin. Lvpruning: An effective yet simple language-guided vision token pruning approach for multi-modal large language models. In *2024 Annual Conference of the North American Chapter of the Association for Computational Linguistics*, 2025.

[49] Xudong Tan, Peng Ye, Chongjun Tu, Jianjian Cao, Xiaoxin Yang, Lin Zhang, Dongzhan Zhou, and Tao Chen. Tokencarve: Information-preserving visual token compression in multimodal large language models. *arXiv preprint arXiv:2503.10501*, 2025.

[50] Gemini Team. Gemini: A family of highly capable multimodal models, 2025.

[51] Oriol Vinyals, Alexander Toshev, Samy Bengio, and Dumitru Erhan. Show and tell: A neural image caption generator. In *2015 IEEE Conference on Computer Vision and Pattern Recognition (CVPR)*, pages 3156–3164, 2015.

[52] Ao Wang, Fengyuan Sun, Hui Chen, Zijia Lin, Jungong Han, and Guiguang Ding. [cls] token tells everything needed for training-free efficient mllms. *arXiv preprint arXiv:2412.05819*, 2024.

[53] Long Xing, Qidong Huang, Xiaoyi Dong, Jiajie Lu, Pan Zhang, Yuhang Zang, Yuhang Cao, Conghui He, Jiaqi Wang, Feng Wu, and Dahu Lin. Conical visual concentration for efficient large vision-language models. In *Proceedings of the IEEE/CVF Conference on Computer Vision and Pattern Recognition (CVPR)*, pages 14593–14603, June 2025.

[54] Dejing Xu, Zhou Zhao, Jun Xiao, Fei Wu, Hanwang Zhang, Xiangnan He, and Yueteng Zhuang. Video question answering via gradually refined attention over appearance and motion. In *Proceedings of the 25th ACM international conference on Multimedia*, pages 1645–1653, 2017.

[55] Senqiao Yang, Yukang Chen, Zhuotao Tian, Chengyao Wang, Jingyao Li, Bei Yu, and Jiaya Jia. Visionzip: Longer is better but not necessary in vision language models. In *Proceedings of the Computer Vision and Pattern Recognition Conference*, pages 19792–19802, 2025.

[56] Weihao Ye, Qiong Wu, Wenhao Lin, and Yiyi Zhou. Fit and prune: Fast and training-free visual token pruning for multi-modal large language models. In *Proceedings of the AAAI Conference on Artificial Intelligence*, volume 39, pages 22128–22136, 2025.

- [57] Xubing Ye, Yukang Gan, Yixiao Ge, Xiao-Ping Zhang, and Yansong Tang. Atp-llava: Adaptive token pruning for large vision language models. In *Proceedings of the Computer Vision and Pattern Recognition Conference*, pages 24972–24982, 2025.
- [58] Hao Yin, Guangzong Si, and Zilei Wang. Lifting the veil on visual information flow in mllms: Unlocking pathways to faster inference. In *Proceedings of the IEEE/CVF Conference on Computer Vision and Pattern Recognition (CVPR)*, pages 9382–9391, June 2025.
- [59] Weihao Yu, Zhengyuan Yang, Linjie Li, Jianfeng Wang, Kevin Lin, Zicheng Liu, Xinchao Wang, and Lijuan Wang. Mm-vet: evaluating large multimodal models for integrated capabilities. In *Proceedings of the 41st International Conference on Machine Learning*, pages 57730–57754, 2024.
- [60] Qizhe Zhang, Aosong Cheng, Ming Lu, Renrui Zhang, Zhiyong Zhuo, Jiajun Cao, Shaobo Guo, Qi She, and Shanghang Zhang. Beyond text-visual attention: Exploiting visual cues for effective token pruning in vlms. In *IEEE/CVF International Conference on Computer Vision (ICCV) 2025*, 2025.
- [61] Qizhe Zhang, Mengzhen Liu, Lichen Li, Ming Lu, Yuan Zhang, Junwen Pan, Qi She, and Shanghang Zhang. Beyond attention or similarity: Maximizing conditional diversity for token pruning in MLLMs. In *The Thirty-ninth Annual Conference on Neural Information Processing Systems*, 2025.
- [62] Shaolei Zhang, Qingkai Fang, Zhe Yang, and Yang Feng. LLaVA-mini: Efficient image and video large multimodal models with one vision token. In *The Thirteenth International Conference on Learning Representations*, 2025.
- [63] Yuan Zhang, Chun-Kai Fan, Junpeng Ma, Wenzhao Zheng, Tao Huang, Kuan Cheng, Denis A Gudovskiy, Tomoyuki Okuno, Yohei Nakata, Kurt Keutzer, and Shanghang Zhang. SparseVLM: Visual token sparsification for efficient vision-language model inference. In *Forty-second International Conference on Machine Learning*, 2025.
- [64] Deyao Zhu, Jun Chen, Xiaoqian Shen, Xiang Li, and Mohamed Elhoseiny. Minigpt-4: Enhancing vision-language understanding with advanced large language models. In *The Twelfth International Conference on Learning Representations*, 2024.
- [65] Jiedong Zhuang, Lu Lu, Ming Dai, Rui Hu, Jian Chen, Qiang Liu, and Haoji Hu. St3: Accelerating multimodal large language model by spatial-temporal visual token trimming. In *Proceedings of the AAAI Conference on Artificial Intelligence*, volume 39, pages 11049–11057, 2025.